

Interaction of phosphine with Si(100) from core-level photoemission and real-time scanning tunneling microscopy

Deng-Sung Lin,* Tsai-Shuan Ku, and Ru-Ping Chen

Institute of Physics, National Chiao-Tung University, 1001 Ta-Hsueh Road, Hsinchu 300, Taiwan

(Received 7 June 1999)

In this paper, we investigate the interaction of phosphine (PH_3) on the Si(100)- 2×1 surface at temperatures between 635 and 900 K. The hydrogen desorption, growth mode, surface morphology, and chemical composition and ordering of the surface layer are examined by synchrotron radiation core-level photoemission and real-time high-temperature scanning tunneling microscopy. The P $2p$ core-level spectra indicate that decomposition of PH_n is complete above ~ 550 K and the maximum P coverage is strongly influenced by the growth temperature, which governs the coverage of H-terminated sites. The scanning tunneling microscopy (STM) images taken at real time during PH_3 exposure indicate that a surface phosphorus atom readily and randomly displaces one Si atom from the substrate. The ejected Si diffuses, nucleates, and incorporates itself into islands or step edges, leading to similar growth behavior as that found in Si chemical vapor deposition. Line defects both perpendicular and parallel to the dimer rows are observed on the nearly P-saturated surface. Perpendicular line defects act as a strain relief mechanism. Parallel line defects result from growth kinetics. STM images also indicate that incorporating a small amount of phosphorus eliminates the line defects in the Si(100)- $2\times n$ surface.

I. INTRODUCTION

In chemical vapor deposition (CVD), phosphine (PH_3) is most frequently used as the phosphorus source gas because of its chemical simplicity. In applications involving silicon integrated circuits, phosphine is commonly added to the Si source gas for *in situ* n -type doping during the deposition.¹ The interaction of phosphine with Si(100) surfaces represents a seemingly simple CVD system and has received much attention.²⁻¹⁰ Many different techniques, including secondary ion mass spectroscopy,² Auger electron spectroscopy,^{2,5,9} x-ray photoelectron spectroscopy,^{3,8} temperature programmed desorption (TPD),^{3,6,9} low-energy electron diffraction,² Fourier transform infrared spectroscopy,⁷ high-resolution electron energy loss spectroscopy,⁶ scanning tunneling microscopy (STM),^{4,5,8,10} and synchrotron core-level photoemission¹⁰ have been employed to study the interaction between phosphine and the Si(100)- 2×1 surface. Cumulatively, the results suggest the following overall thermal reaction pathways: (1) phosphine initially molecularly adsorbs on one side of a dimer at room temperature with a sticking coefficient of near unity. The adsorbed PH_3 radical dissociates into PH_2 at low coverage over a period of minutes. At a higher coverage (≥ 0.18 ML, 1 ML = 6.78×10^{14} cm^{-2}), only a small amount of adsorbed PH_3 is converted to PH_2 owing to the lack of nearby surface dangling bonds (DB's). (2) The conversion of the remaining adsorbed PH_3 to PH_2 is completed at less than 620 K, and that of PH_2 to P is completed at less than 700 K. The actual reaction temperature strongly depends on the availability of surface DB for releasing H. (3) The total phosphorus coverage is 0.37 ML on a PH_3 -saturated Si(100) surface at room temperature, but is reduced to a nominal 0.25 ML upon annealing to 700 K via the desorption of PH_3 . This phenomenon occurs because surface sites of three times of that coverage (0.75 ML) are

consumed by dissociated hydrogen. (4) The final state of a phosphine-saturated Si(100) surface after complete H desorption is a random alloy of Si-P and Si-Si dimers.

Regarding the growth of P at different substrate temperatures, the maximum coverage of P is found to vary strongly with substrate temperature, ~ 0.25 ML at ~ 650 K and ~ 1 ML at ~ 800 K.^{2,8,10} Using the conventional, "growth-interruption-observation" STM, Wang, Chen, and Hamers found that surface phosphorus atoms displace Si from the substrate at 825 K and form predominantly Si-P heterodimers uniformly on the surface over a wide range of P coverages.⁵ They also reported large numbers of stress-induced line defects perpendicular to the dimer rows on the P-terminated Si(100) surface. Also, Kipp *et al.* observed a strong tendency for missing dimer rows to be formed parallel to the P dimer rows.⁸ The researcher's total-energy calculations suggested large tensile stresses for the P-terminated Si(100) surface in both directions rather than for bared Si(100)- 2×1 surface. This finding suggests that stress relief is the driving force for the defect lines and that all the vacancy lines either parallel or perpendicular to dimer rows consist of P passivated Si(111) microfacets.

In light of the above developments, this study presents synchrotron radiation core-level photoemission spectroscopy and STM data for the thermal interaction of phosphine and growth of phosphorus on Si(100)- 2×1 in the temperature range of 635–900 K. The images of variable-temperature scanning tunneling microscopy revealed in real time the evolution of surface morphology during phosphorus CVD in atomic resolution, thereby providing comprehensive insight into the growth processes which occur on the Si(100) surface. Experimental results indicate that the growth of phosphorus on Si(100) using phosphine involves H termination at less than 640 K, island growth at ~ 700 K, and step flow growth at 800–900 K. These growth features are similar to

those found in Si CVD using Si_2H_6 , because Si, ejected by P from the substrate, diffuses, nucleates, and incorporates itself into steps.

II. EXPERIMENTAL DETAILS

STM measurements were performed in a stainless-steel chamber with a base pressure less than 1×10^{-10} torr. A bolt-on commercial variable temperature UHV-STM system was used. The STM tips were electrochemically etched tungsten wires. All images were obtained in a constant current mode with a tunneling current of ~ 0.3 nA. Distortions due to thermal drift were not corrected. The photoemission experiments were performed in another μ -metal shielded UHV system utilizing 1.5-GeV synchrotron radiation in the Taiwan Light Source, Hsinchu, Taiwan. Light from the storage ring was dispersed by a 6-m low-energy spherical grating monochromator. The photocurrent from a gold mesh positioned in the synchrotron beam path was monitored to relatively measure the incident photon beam flux. The PH_3 adsorption, annealing, and phosphorus growth were prepared *in situ* in UHV conditions. Photoelectrons were collected and analyzed by a 125-mm hemispherical analyzer. The overall energy resolution was less than 120 meV. The Si(100) samples were sliced from boron-doped wafers with a dopant concentration of approximately $1.5 \times 10^{15} \text{ cm}^{-3}$. The wafer's misalignment was around 0.1° towards [011]. After outgassing at 900 K for 12 h, the clean Si(100)- 2×1 sample is obtained by dc joule heating to 1450 K. Phosphine (Voltaix, ultrahigh purity grade) was introduced into the chamber through a precision leak valve. The dosing pressure was around 1×10^{-8} torr with the ion pumping running in all measurement. The substrate temperature was varied by controlling the dc current through the sample and measured with an infrared pyrometer.

III. RESULTS AND DISCUSSION

A. Photoemission measurement on the phosphorus growth

Figure 1 displays the P $2p$ core-level spectra for the Si(100) surface after exposure to 15 L (1 L = 10^{-6} Ts) of phosphine at various substrate temperatures. The dosing pressure (1×10^{-8} torr) was the same as that used for taking other STM measurements reported in this study for direct comparison. The binding energy scale is referred to the corresponding bulk component of the Si $2p$ line (not shown here). Adopting this energy reference removes the effect of band bending induced by changing surface conditions.¹⁰ The P $2p$ spectrum for the 300 K phosphine-saturated Si(100) surface exhibits two spin-orbit-split components, labeled $P3$ and $P2$ in Fig. 1. Previous investigations showed that the adsorbed PH_3 partially decomposes to form PH_2 by releasing a hydrogen atom to a nearby Si DB and that the $P3$ and $P2$ components correspond to the emissions from the adsorbed PH_3 and PH_2 surface species, respectively.¹⁰ The remaining spectra in Fig. 1 essentially exhibit only one spin-orbit-split component, suggesting the absence of PH_n ($n=1,2,3$) species on the surface at these growth temperatures. The normalized integrated intensities of P $2p$ spectra in Fig. 1 account for the relative abundance of surface phosphorus atoms at various adsorption temperatures, and are plotted in

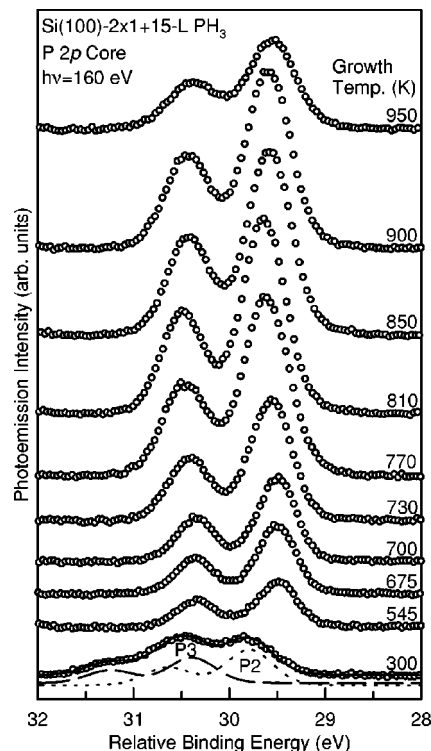


FIG. 1. P $2p$ core-level photoemission spectra (circles) for 15-L phosphine adsorption on Si(100) at various growth temperatures as indicated. The curves labeled $P2$ and $P3$ are the results of decomposition for the bottom spectrum into individual components, each having a pair of spin-orbit-split peaks. To eliminate the band bending effect, the relative binding energy for P $2p$ refers to the corresponding Si $2p_{3/2}$ line of the bulk component (not shown). The overall energy resolution was less than 120 meV.

Fig. 2. The intensity of the maximum coverage is nominally 1 ML, as indicated in Refs. 2 and 8. As Fig. 2 reveals, the maximum coverage of P is only ~ 0.25 at around 600 K, due to the presence of 0.75-ML H from decomposition of PH_3 . Above ~ 680 K, the coverage abruptly increases and reaches a maximum of 1 ML between ~ 770 and 900 K. The desorption rate of P from the surface becomes significant above 900 K and the coverage of P decreases for the same PH_3 dosing

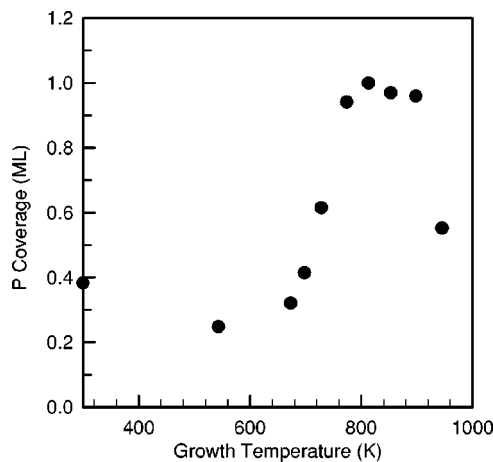


FIG. 2. Phosphorus coverage, obtained from the integrated P $2p$ core-level intensity in Fig. 1, as a function of growth temperature.

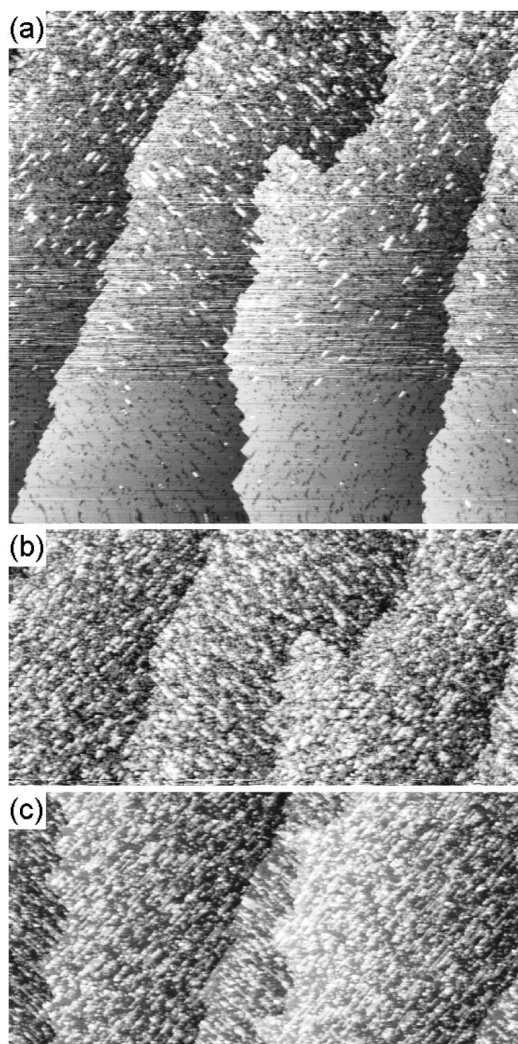


FIG. 3. Real-time STM images of Si(100) dosed by (a) 0.7, (b) 2, and (c) 10 L of phosphine at 640 K. The noisy lines in the middle of (a) resulted from the vibration that occurred while the leak valve was being opened. The images are of size (a) $2000 \times 2000 \text{ \AA}^2$ and (b),(c) $2000 \times 1000 \text{ \AA}^2$. The sample bias is -2 V ; the tunneling current was 0.3 nA .

pressure. The temperature dependence of P coverage will be further discussed in conjunction with STM observation in the following sections.

B. Phosphorus and hydrogen passivation at $T=640 \text{ K}$

Figure 3 illustrates the real-time observation of the phosphine interaction with Si(100) at 640 K, a temperature well below the $\beta_1 \text{ H}_2$ desorption peak (800 K) from a Si(100)- 2×1 :H surface.¹¹ During scanning, the clean Si(100)- 2×1 surface is maintained at 640 K and continuously exposed to phosphine. The accumulative exposures at the top of Figs. 3(a), 3(b), and 3(c) are about 0.7, 2, and 10 L, respectively. Since the shadowing effect of the tips could effectively reduce the gas impingement rates by more than 50% during real-time imaging,¹² the exposure on the surface is not accurately known. The noisy lines in the middle of Fig. 3(a) resulted from the vibration that occurred while the leak valve was being opened. The primary features at the bottom of Fig.

3(a) denote alternatively smoother and rougher steps (so-called S_A and S_B , respectively) before dosing. Soon after exposure began, one-dimensional (1D) chains orthogonal to the substrate dimer rows appeared on the terraces. According to the P $2p$ spectra in Fig. 1, dissociation of hydrogen is completed at this temperature. As estimated, the surface residential time for hydrogen on Si_2H_2 monohydride dimers at this temperature is more than 4000 s from a previous measurement.¹³ Hence, hydrogen dissociated from the adsorbed PH_3 radicals initially remains on the surface, attaches to nearby Si DB's, diffuses on the surface, and forms Si_2H_2 monohydride dimers upon encountering other unpaired surface H atoms. The monohydride dimers thus formed can be observed as dark spots in the upper half of Fig. 3(a), since their apparent height is lower than that of clean Si dimers. Figures 3(b) and 3(c) indicate that the surface was nearly saturated after 2-L exposure and its morphology remains largely the same afterwards. This is expected since both H and P terminate surface DB's and ultimately prevent further PH_3 adsorption. To examine the details of atomic ordering at the surface, growth was terminated after 12-L exposure and the sample was cooled to room temperature to prevent further surface reaction. Figure 4 displays the dual-voltage images of the surface taken at room temperature. The empty state image [Fig. 4(b)] closely resembles that of hydrogen terminated Si(100)- 2×1 :H obtained by disilane (Si_2H_6) saturation exposure at a similar substrate temperature: both the Si chains and substrate dimer rows show well ordered 2×1 periodicity.¹² In contrast, the same dimer rows appear to wobble in the filled state image [Fig. 4(a)], indicating that there is lack of ordering in chemical composition. Since P is a group V element, a P-Si-H surface species and a P-P dimer exhibit similar filled state tunneling environments with a H-Si-Si-H monohydride dimer. This leads us to infer that the P atoms are, in fact, randomly dispersed on both the chains and the substrate surface in the form of either H-Si-P or P-P dimers. The chains not only consist of adsorbed P atoms but also of Si ejected from the substrate. Notably, the coverage of chains in Fig. 3(c) is nominally 0.25 ML, a value that corresponds well with the photoemission calibration in Fig. 2 and the fact that dissociated H passivates the other 0.75 ML of surface DB's. It is thus clear that one P atom displaces only one Si atom from the substrate.

In Fig. 4, some bright protrusions are evident. Their characteristic nodal patterns in the empty state image [Fig. 4(b)] indicate that they are Si DB pairs formed by H_2 desorption. The generation of DB pairs due to hydrogen desorption becomes more visible in Fig. 5: the coverage of DB pairs increases on the surface after 12-L PH_3 exposure at 635 K was maintained at the same temperature without further PH_3 exposure. Figure 6 plots the coverages of DB pairs on both the substrate and the chains as a function of annealing time. This figure indicates that the total coverage of DB pairs after 871-min annealing is only $\sim 0.43 \text{ ML}$. This value is much smaller than 0.75 ML, the surface hydrogen coverage after 12-L saturation exposure. Hence, there remains 0.32 ML of hydrogen on the surface. As photoemission data in Sec. III A suggest, this growth condition contains a nominal 0.25 ML phosphorus on the surface. Furthermore, previous investigations confer that P-Si heterodimers are energetically favorable for submonolayer P coverage.⁵ All these considerations

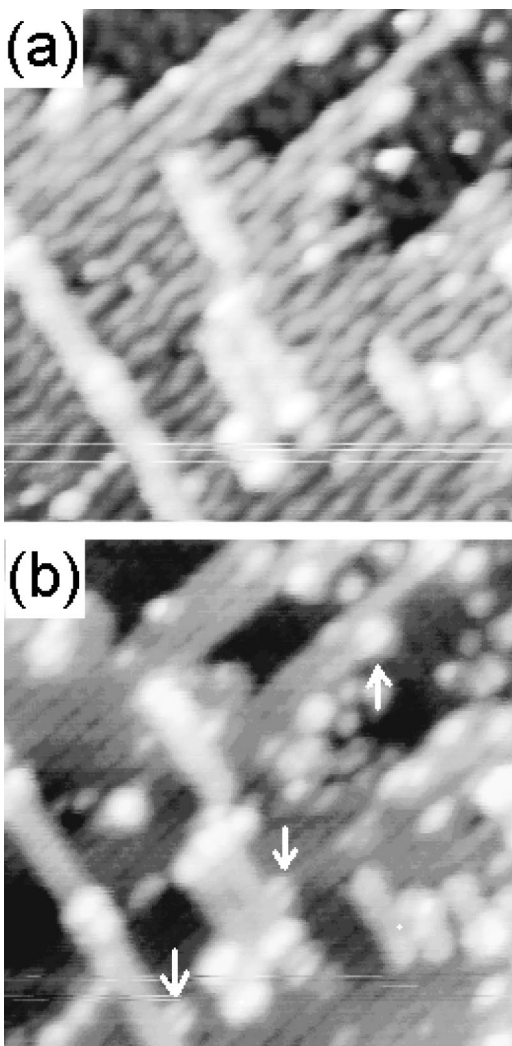


FIG. 4. Dual-voltage STM images ($\sim 163 \times 163 \text{ \AA}^2$) of the Si(100) surface after 12-L PH_3 exposure at 640 K. The (a) filled state and (b) empty state images were taken at room temperature at sample biases of -2.0 and $+2.0$ V, respectively. The tunneling current was 0.3 nA. The arrows in (b) indicate characteristic nodal patterns of Si DB pairs produced by H_2 desorption from the monohydride dimers.

together suggest that the apparent darker sites between DB pairs, accounting for 0.57 ML, consist mainly of (~ 0.5 ML) P-Si-H dimers and some (~ 0.07 ML) Si_2H_2 monohydride dimers. Figure 6 also demonstrates that the desorption rate of hydrogen eventually becomes very small, although the total hydrogen coverage is still high. This finding is expected since the H_2 recombinative desorption from two P-Si-H dimers involves other complications: hydrogen in P-Si-H dimers must diffuse from site to site and undergoes a collision leading to reaction and molecular desorption. Notably, the DB pairs in Figs. 5(b) and 5(c) do not form large islands, even though they are rather free to move on the surface at this temperature. Instead, the DB pairs, particularly those on the chains in Fig. 5(c), apparently keep a distance ($2a_0$, $a_0 = 3.84 \text{ \AA}$) from each other. Since PH_3 adsorption is random, the regular distribution of DB pairs is unlikely owing to the regular distribution of Si_2H_2 and P-P dimers. The image such as that in Fig. 5(c) appeared stable for hours, indicating that the surface is nearly a thermodynamically favorable configura-

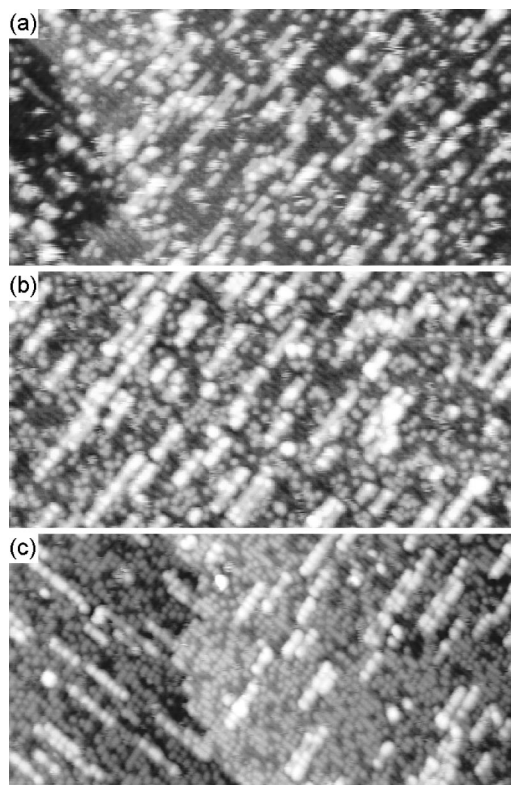


FIG. 5. Filled-state STM images showing H_2 thermal desorption. The Si(100) surface was exposed to 12-L PH_3 at 635 K and subsequently annealed at the same temperature without PH_3 flux for (a) 40, (b) 164, and (c) 667 min, respectively. The areas are $\sim 560 \times 280 \text{ \AA}^2$. The bright protrusions are DB pairs.

tion. Reference 13 suggests that this phenomenon may be due to Coulomb repulsion between DB pairs.

C. Two-dimensional nucleation growth at $T=690$ K

Figure 7 displays the selected STM images of the Si(100) surface which was maintained at 690 K during exposure to phosphine. This temperature is still below but closer to the β_1 H_2 desorption peaks in TPD than 640 K. At this temperature, the residential time of surface hydrogen is in the order of minutes. The initially clean Si(100)- 2×1 surface [Fig. 7(a)] has a low concentration of dimer vacancies, which ap-

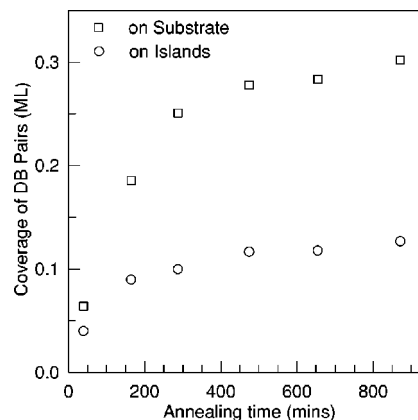


FIG. 6. Coverage of DB pairs counted from STM images as a function of annealing time at 635 K.

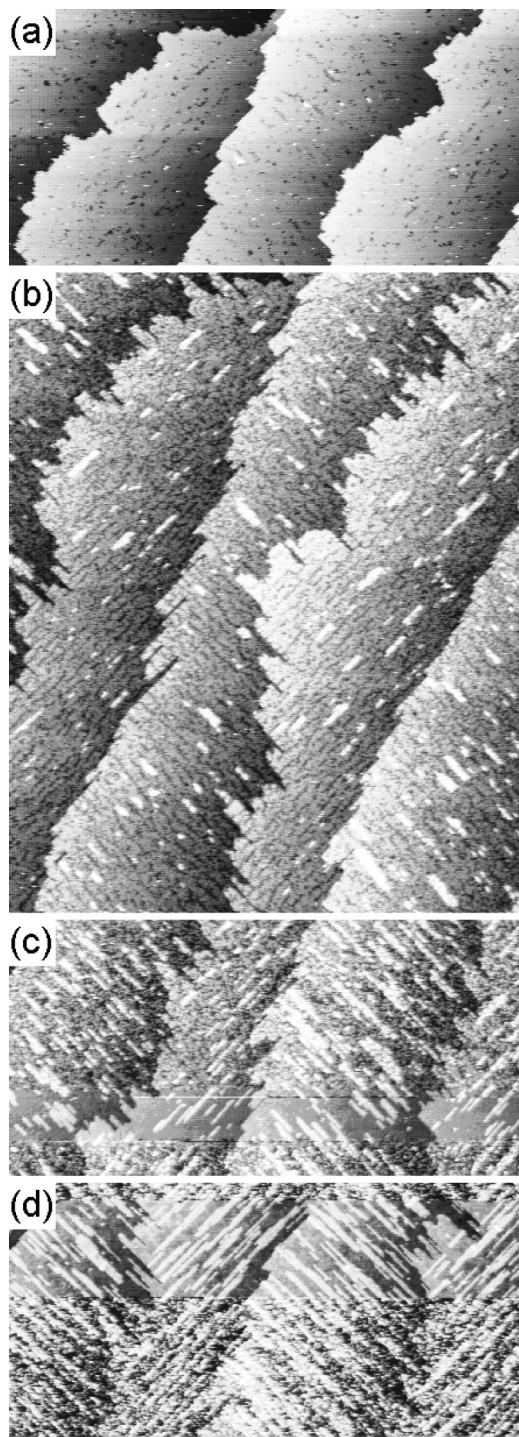


FIG. 7. (a) STM images of the initial Si(100)- 2×1 surface. (b)–(d) Images obtained in real time after the surface in (a) is exposed to (b) 1, (c) 6, and (d) 12 L of phosphine. All images are recorded at 690 K. The sample bias was -2.0 V; the tunneling current was 0.3 nA. The image sizes are 2000×2500 Å² for (b) and 2000×1000 Å² for (a), (c), and (d).

appear as dark spots. Upon exposure to phosphine, small 2D islands appear and grow on the terraces as shown in Fig. 7(b), along with dark spots. Denuded zones (striped areas with no nucleated islands) can also be observed around the S_B step edges in Fig. 7(b). These occurrences of denuded zones resemble those in Si molecular beam epitaxy.¹⁴ As mentioned in Sec. III B, most P after complete H dissociation

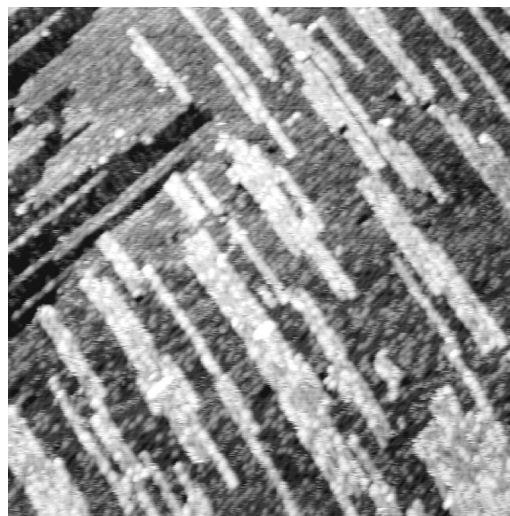


FIG. 8. Filled-state STM images taken 4 min after the Si(100) was exposed to 13.4-L phosphine at 690 K.

readily displace Si from the substrate at low coverage. Ejected Si diffuses on the dimerized surface before nucleating into islands. Therefore, the growth processes and the resulting surface morphology at low coverage resemble those of Si MBE. Figure 7(b) shows two kinds of dark spots. The first is randomly dispersed on the substrate: they are either Si-P heterodimers, or Si₂H₂ monohydride dimers, or P-Si-H dimers. The second forms short 1D trains and is only seen in the initial stage of exposure shown in the lower half of Fig. 7(b). The 1D chains exhibit a lower apparent height (darker) than the first kind and resemble the missing dimer chains seen on a clean Si(100)- 2×1 surface.¹⁵ Since the 1D defect trains are not observed in the P- and H-saturated Si(100) systems,^{5,16} they can be temporarily considered to be adsorbate-induced missing dimer lines. As the growth proceeds, the 2D islands also slowly increase their density [Fig. 7(c)] and grow in size [Fig. 7(d)], indicating the continued phosphine adsorption. In both Figs. 7(c) and 7(d), the tip changed twice, resulting in a band in each of the two images. The surface areas in the bands appear smoother, although their chemical homogeneity is the same as seen in other areas. The gas valve was closed after 13.4-L exposure. The surface morphology after 4-min annealing at the constant temperature is shown in Fig. 8. After 4 min of annealing, the amount of surface H is expected to be small and the surface is a partially P-terminated surface. The 2D islands and the substrate have the same structure of dimer rows with random bright protrusions. Since Si atoms exhibit a greater apparent height than P atoms,⁵ the bright protrusions randomly dispersed on both the islands and the substrate are presumably Si atoms. Both the islands and the substrate consist of a mixture of Si and P, as evidenced by the homogeneity of Si distribution. The island coverage is estimated to be about 0.43 ML and expected to increase continuously with exposure. In Fig. 2, the P coverage for 15-L phosphine exposure at 1×10^{-8} torr exhibits a slope between 680 and 780 K. In this temperature range, the surface H concentration during growth declines exponentially with temperature. In other words, the number of available DB's for PH₃ adsorption increases rapidly with temperature, resulting in the slope in P coverage at a constant dosing pressure and duration.

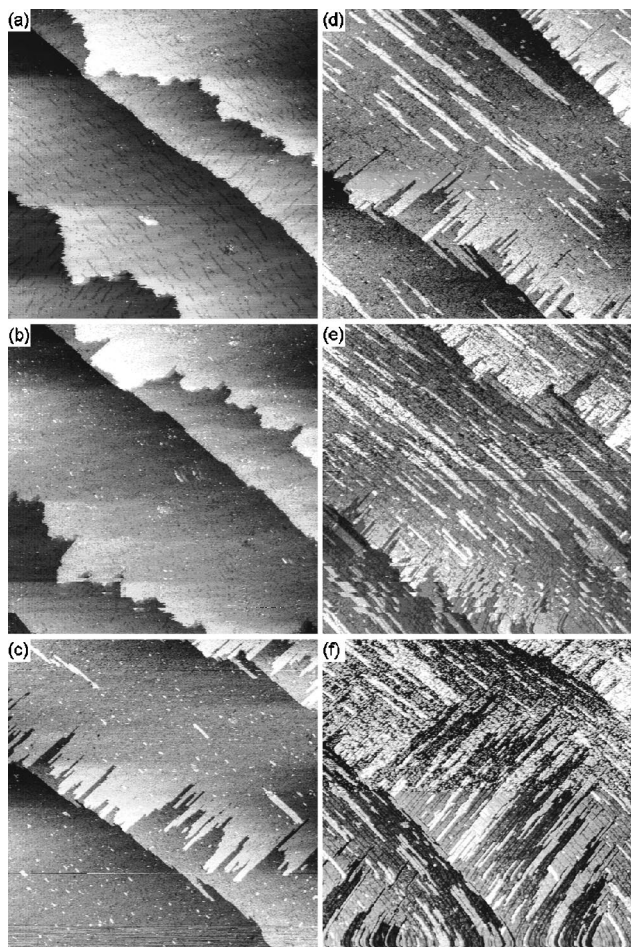


FIG. 9. Real-time STM images ($2000 \times 2000 \text{ \AA}^2$) of Si(100) dosed by (a) 0.5, (b) 1, (c) 1.5, (d) 3, (e) 4, and (f) 10 L of phosphine at 800 K. The sample bias was -2 V ; the tunneling current was 0.3 nA .

D. Step-flow growth at $T=800\text{--}900 \text{ K}$

Figures 9(a)–9(f), taken at 800 K, illustrate the typical growth behavior of P on the Si(100) surface in the temperature range of 800–900 K. Above 800 K, H desorbs immediately upon phosphine adsorption and dissociation and, in such a case, the surface coverage of H is nearly zero. The net effect is continuous phosphorus deposition until the entire surface is eventually passivated. Showing clear 2×1 dimer reconstruction, the passivated surface (Fig. 10) has a maximum P coverage of nominal 1 ML because there are no more DB's for further phosphine adsorption. At the temperature range of 800–900 K, the adsorbed P and/or displaced Si adatoms left behind after H desorption are mobile enough to reach the step edges, leading to step-flow growth [Figs. 9(a) and 9(b)]. As mentioned earlier, P exhibits substantially lower than Si. If only adsorbed P were responsible for the step flow, the growth areas at the step edge would appear darker than the terraces before growth. However, all areas in Fig. 9 appear the same, indicating that the chemical composition is about the same all over the surface, and suggesting that the growth of P proceeds by a steady increase in the proportion of P throughout the entire surface. At low coverage, most of the P atoms are expected to displace Si atoms

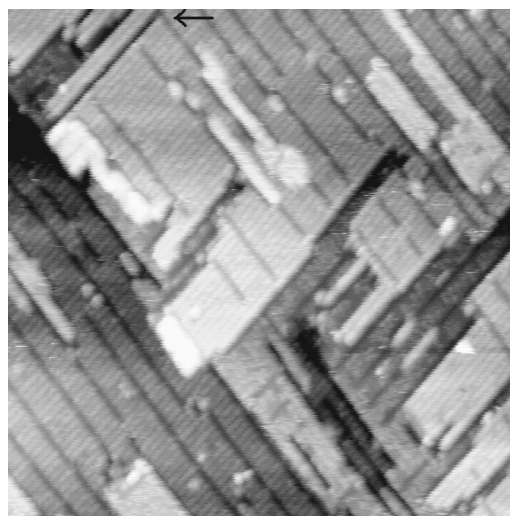


FIG. 10. STM images ($520 \times 520 \text{ \AA}^2$) of P-passivated Si(100) recorded at 800 K. The black arrow points at one of the line defects parallel to dimer rows. The sample bias is -2 V .

on the terrace before traveling far. The ejected Si diffuses on the surface and eventually is incorporated into step edges. This scenario closely resembles the Si homoepitaxy. Previous studies concluded that the rate of Si incorporation into S_B steps is markedly higher than that into S_A steps.^{14,17} Naturally, the S_B steps advance faster than S_A steps, leading to the formation of a nearly single-domain surface, as Figs. 9(c) and 9(d) display. As the phosphine dosage increases, phosphorus accumulates and very anisotropic 2D islands begin to form on the terraces, as are shown in Figs. 9(d), 9(e), and 9(f). Phosphorus terminates the surface dangling bonds on dimers: an effect similar to that of hydrogen termination. It is likely that, as on the partial H-terminated Si(100) surface,¹⁸ the effective barrier for Si diffusion is significantly higher on a partial P-covered Si(100) surface than on a clean Si(100) surface.

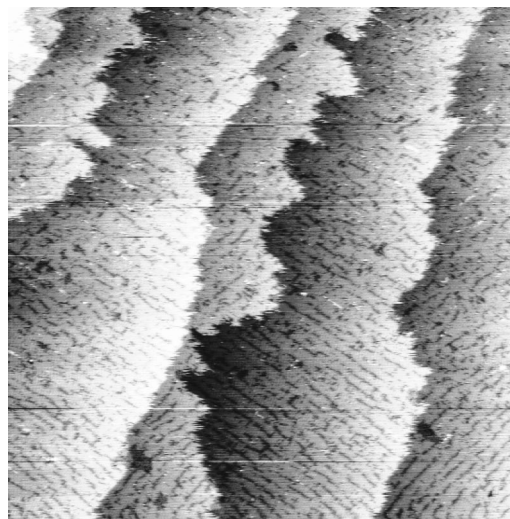


FIG. 11. Real-time STM images ($2000 \times 2000 \text{ \AA}^2$) of Si(100) dosed by 0.1 (bottom), -0.7 (top) L of phosphine at 900 K. The initial surface is Si(100)- $2 \times n$ obtained by annealing a clean Si(100)- 2×1 surface for 5 h at 900 K. The defect lines at the lower half gradually disappear as P coverage increases.

The P-passivated surface (Fig. 10) contains large numbers of line defects perpendicular to the dimer rows. This finding accords with previous observation.^{5,8} The defects were interpreted as acting as a stress relief mechanism. Near the step edges, there are also some missing dimer rows parallel to the P-P dimer rows. Figures 9(c)–9(f) reveal that the S_B steps advance via finger growth. Also, the 2D islands on the terrace are very anisotropic. These observations suggest that the rate of incorporation of Si or P dimers onto the end of dimer rows is markedly higher than that of their incorporation into the side.¹⁴ Between growth fingers near steps, there appear missing dimer rows parallel to the dimer rows. The images strongly suggest that the formation of parallel missing dimer rows is not due to energy minimization,⁸ but to growth kinetics.

In Fig. 9(a), the short missing dimer chains in the lower half, arising from elevated-temperature annealing before PH_3 exposure,¹⁹ gradually disappear as the scan went from bottom to top. This observation had been reproduced several times at the temperature range of 800–900 K. Figure 11 illustrates one of the experiments. A Si(100)- $2 \times n$ surface was produced by annealing a clean Si(100)- 2×1 surface at 900 K for several hours, following the method described in a previous report.¹⁹ The $2 \times n$ pattern clearly shown in the lower half rapidly disappears as the PH_3 dose increases to a value of 0.7 L at the top. One might suggest that phosphorus fills the defect lines. However, closely examining the surface does not reveal any sign of P-P dimer lines (expected to appear darker than surrounding Si), ruling out this possibility. Although the mechanism responsible for eliminating the $2 \times n$ defect structure requires further theoretical study, a low concentration of P on the Si(100) surface obviously reduces the driving force behind the formation of the $2 \times n$ structure.^{15,20}

IV. SUMMARY

By combining real-time atomic-scale microscopy and core-level photoemission spectroscopy techniques, this work further elucidates the kinetic processes which occur during phosphine exposure on a Si(100) surface. Although this is one of the simplest CVD systems available, our real-time STM images reveal many complex surface reactions. After PH_3 exposure of more than 10 L, the Si(100) surface is passivated by H and/or P. The P coverage depends on the H surface residential time at the growth temperature. A surface phosphorus atom readily and randomly displaces one Si atom from the substrate and the ejected Si diffuses, nucleates, and is incorporated into islands or step edges. Consequently, the growth behavior, such as H termination at ~ 640 K, island formation at ~ 700 K, and step flow at 800 K, is found to be similar to that found in Si chemical vapor deposition. Line defects both perpendicular and parallel to the dimer rows are observed on the nearly P-saturated surface. Perpendicular line defects acts as a strain relief mechanism. Parallel line defects are a result of growth kinetics. Real-time STM images also indicate that incorporating small amount of phosphorus eliminates the line defects in the Si(100)- $2 \times n$ surface.

ACKNOWLEDGMENTS

This work was supported by the National Science Council, Taiwan, under Contract No. NSC88-2112-M009-005. The authors gratefully acknowledge L. J. Lauhon, H. Lee, and W. Ho for their assistance and discussions. D.S.L. wishes to thank the Laboratory of Atomic and Solid State Physics, Cornell University, for its hospitality during the preparation of this manuscript.

*Electronic address: dslin@cc.nctu.edu.tw

¹See, for example, C. W. Pearce, in *VLSI Technology*, edited by S. M. Sze (McGraw-Hill, New York, 1983) Chap. 2.

²M. L. Yu and B. S. Meyerson, *J. Vac. Sci. Technol. A* **2**, 446 (1984).

³M. L. Yu, J. J. Vitkavage, and B. S. Meyerson, *J. Appl. Phys.* **59**, 4032 (1986).

⁴Y. Wang, M. J. Bronikowski, and R. J. Hamers, *J. Phys. Chem.* **98**, 5966 (1994).

⁵Y. Wang, X. Chen, and R. J. Hamers, *Phys. Rev. B* **50**, 4534 (1994).

⁶M. L. Colaianni, P. J. Chen, and J. T. Yates, Jr., *J. Vac. Sci. Technol. A* **12**, 2995 (1994).

⁷J. Shan, Y. Wang, and R. J. Hamers, *J. Phys. Chem.* **100**, 4961 (1996).

⁸L. Kipp, R. D. Brigans, D. K. Biegelsen, J. E. Northrup, A. Garcia, and L. E. Swartz, *Phys. Rev. B* **52**, 5843 (1995).

⁹M. L. Jacobson, M. C. Chiu, and J. E. Crowell, *Langmuir* **14**,

1428 (1998).

¹⁰D.-S. Lin, T.-S. Ku, and T.-J. Sheu, *Surf. Sci.* **424**, 7 (1999).

¹¹K. Sinniah, M. G. Sherman, L. B. Lewis, W. H. Weinberg, J. T. Yates, Jr., and K. C. Janda, *J. Chem. Phys.* **92**, 5700 (1990).

¹²P.-H. Wu and D.-S. Lin, *Phys. Rev. B* **57**, 12 421 (1998).

¹³D.-S. Lin and R.-P. Chen, *Phys. Rev. B* **60**, R8461 (1999).

¹⁴Y.-W. Mo and M. G. Lagally, *J. Cryst. Growth* **111**, 876 (1991); Y.-W. Mo, R. Kariotis, B. S. Swartzentruber, M. B. Webb, and M. G. Lagally, *J. Vac. Sci. Technol. A* **8**, 201 (1990).

¹⁵H. J. W. Zandvliet, *Surf. Sci.* **377-379**, 1 (1997).

¹⁶J. J. Boland, *Adv. Phys.* **42**, 129 (1993).

¹⁷B. Voigtlander, T. Weber, P. Smilauer, and D. E. Wolf, *Phys. Rev. Lett.* **78**, 2164 (1995).

¹⁸J. E. Vasek, Z. Zhang, C. T. Salling, and M. G. Lagally, *Phys. Rev. B* **51**, 17 207 (1995).

¹⁹D.-S. Lin and P.-H. Wu, *Surf. Sci. Lett.* **397**, 273 (1998).

²⁰F. K. Men, A. R. Smith, K. J. Chao, Z. Zhang, and C. K. Shih, *Phys. Rev. B* **52**, 8650 (1995).